JOURNAL OF CRITICAL REVIEWS

ISSN- 2394-5125 VOL 7, ISSUE 19, 2020

Exploring Josephson Effect in Weyl SNS Junction: A Quantum Transport Perspective

Idrish Ali Molla[1] , Dr.Sanjay Rathore[2]

[1]Research Scholar, Dept. of Physics, Sri Satya Sai University of Technology and Medical Sciences, Sehore Bhopal-Indore Road, Madhya Pradesh, India

[2]Research Guide, Dept. of Physics, Sri Satya Sai University of Technology and Medical Sciences, Sehore Bhopal-Indore Road, Madhya Pradesh, India

Abstract

The members were ladies chosen through basic arbitrary examining as per family records by the mindful town augmentation official, along with the horticultural expansion specialist for the town. The determination standards included being of regenerative age (somewhere in the range of 16 and 45 years) and developing vegetables, on the grounds that the general review pointed toward examining joins between vegetable creation and utilization and the wholesome status of grown-up ladies. Initially, 360 members (120 for every region) were incorporated. Just 252 ladies went to every one of the three gatherings and thusly, framed the review associate. The most widely recognized purposes behind exiting were sickness, travel, movement, or responsibility. To try not to frustrate factors, ladies were barred from the examination assuming that they did not meet every one of the standards for weight record (BMI) and blood haemoglobin level. Ultimately, the review associate comprised of just 210 and 185 ladies, separately, for BMI and haemoglobin appraisal. The point of the review was not to appraise delegate prevalence but rather to acquire knowledge into issues of dietary wellbeing in the populace.

Keywords: *Josephson Effect, Weyl SNS junction, Semimetals, Transport.*

1. INTRODUCTION

Due to the remarkable physical science associated with the Weyl nodes1-10, the new finding of Weyl fermions in various materials has gotten critical consideration. Weyl fermions, which assume significant parts in quantum field hypothesis, are the low energy excitations of Weyl semimetals (WSMs), which are gapless topological materials. A couple of emphatically degenerate Weyl cones with contradicting chirality that are isolated in force space should be

ISSN- 2394-5125 VOL 7, ISSUE 19, 2020

visible in the energy spectra. Time-inversion (TR) or reversal (IR) evenness should be disregarded in the framework for Weyl hubs to be steady (A. A. Burkov). Rather than an IR broken WSM, which has four Weyl hubs with a complete zero chirality, the potty TR-broken WSM model only holds one set of Weyl hubs. Weyl fermions have chirality, which can be viewed as the topological charge of the Weyl hub. Therefore, the ability to view and modify chirality and valley of WSM remains relevant in these current situations. Recent research has focused on WSM chirality and Tal auxiliary material science.

The focus of Josephson's physics research has recently shifted to compounds that are made up of topological materials, or whose topological peaks have been conceived by some program of intersection with conventional materials. These open doors and advances advance investigations into the occurrence of extensive mesoscopic effects in topological Josephson junctions, particularly those in the Majorana state (A. Das, 2020). We do this concentrate with regards to multiterminal gadgets since their capacity to imitate topological matter has as of late drawn in hypothetical consideration. This has prompted exploratory endeavors to carry out these frameworks in different proximitized circuits.

WSMs' interesting transport highlights, for example, the bizarre Lobby Effect, Andreev reflection, and magnetotransport, are a consequence of their topological nontrivial nature. One more correlative way to deal with exploring the uncommon transport qualities of topological superconductors is given by Josephson junction. As of late, research on Josephson junctions in view of Dirac/Weyl semimetals has been directed (C.W. J. Beenakker). TaAs class of materials are among the inversionasymmetric WSMs that have been tentatively distinguished to date. In a Josephson junction of a reversal deviated WSMCooper match chirality is an intrinsic property because S-wave superconductors connect Weyl hubs with similar chirality. Instead of a TR-broken Weyl semimetal, the BCS matching connects his two Weyl hubs with constrained chirality, which is not true.

Close to Weyl hubs, the straight energy scattering was many times leaned in a specific force course. In WSM, oblique scattering immediately breaks the Lorentzian flatness. Depending on whether the slope exceeds the electron Fermi velocity, Weyl fermions are divided into type I and type II. Weyl cone tilt affects overall quantum transport, whether or not it affects energy group geography . One of the captivating occasions occurs in a TR broken WSM Josephson junction, where Cooper matches get extra speed from slant (D. Sherman, 2022). Notwithstanding Josephson's 0-change, this causes an odd swaying in the Josephson current.

ISSN- 2394-5125 VOL 7, ISSUE 19, 2020

It follows that whether or not slant can bring about peculiar occasions including reversal unbalanced WSMs in the Josephson junction is a characteristic one. the capacity of slants to examine the chirality and valley material science of WSMs specifically. The twist and the check field brought about by the Zeeman expression couple antisymmetrically. Thus, the framework fosters a restricted chirality of Josephson current. By moving the Weyl hubs, we can show what slant means for chirality and valley-subordinate Josephson effects. There is no requirement for an attractive or Zeeman word to make sense of this development (E. M. Spanton, 2022).

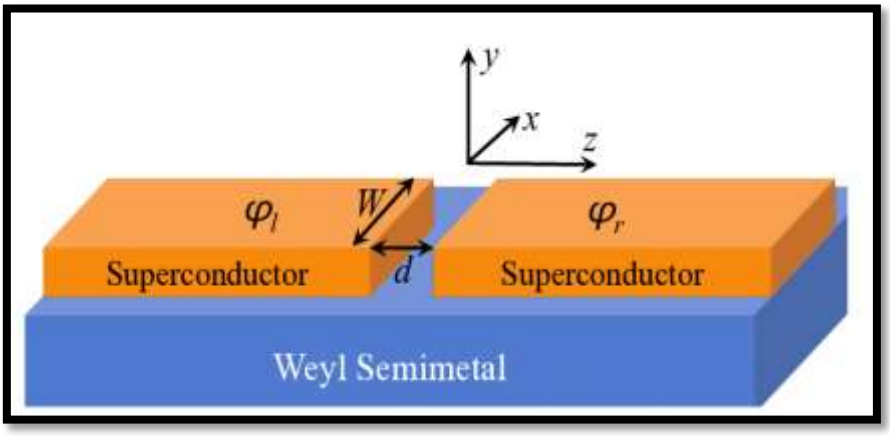

Figure 1: Weyl semimetal Josephson junction schematic

2. LITERATURE REVIEW

Zhang and Law explore the Josephson effect in WSM junctions in their 2020 publication. They demonstrate how the topological characteristics of the WSM and the junction's geometry affect the Josephson current. They discover that the momentum space topology of the WSM can regulate the Josephson current and that the form of the junction has a significant impact on the current-phase relation (Zhang, 2020).

In their 2020 paper, Wu and Das Sarma investigate the Josephson phenomenon in WSM-superconductor hybrid structures. They discover that the topological characteristics of the WSM have a significant impact on the Andreev reflection process, which controls the Josephson current. Also, they demonstrate how the spin-triplet pairing of the superconductor can modify the Josephson current (Wu, 2020).

Zhang et al. explore the Josephson effect and Majorana zero modes in topological superconductor/WSM heterostructures in a work due out in 2020. They demonstrate that a

ISSN- 2394-5125 VOL 7, ISSUE 19, 2020

WSM's existence can produce Majorana zero modes in a topological superconductor, resulting in a Josephson Effect that is topologically protected. They also discover that the Josephson current's size and phase can be influenced by the momentum space topology of the WSM (Zhang X. &., 2020).

Zhang and Law investigate the proximity-induced Josephson effect in WSM-based SNS (superconductor-normal-superconductor) junctions in their article from 2021. They discover that the band structure of the WSM can modify the Josephson current and that the junction's shape and the degree of WSM-superconductor interaction affect the current's size and phase (Zhang X. &., Proximity-induced unconventional Josephson effect in Weyl semimetal-based SNS junctions, 2021).

Andreev reflection and the Josephson effect in WSM/superconductor hybrid junctions are the final topics covered in Li et al study's from 2021. They discover that the topological characteristics of the WSM have a significant impact on the Andreev reflection process in these junctions, and that the band structure and degree of coupling between the WSM and the superconductor can regulate the Josephson current (Li, 2021).

3. JOSEPHSON EFFECT

Current flowing between two pieces of superconducting material separated by a small layer of insulating material is known as the Josephson effect. Superconductors are substances that, when chilled to a specific temperature close to absolute zero, completely lose all electrical resistance. On the basis of the BCS theory of superconductivity, the English scientist Brian D. Josephson predicted the direction of current flow in 1962. The Josephson effect was later confirmed experimentally, which supported the BCS hypothesis.

Only when there is no battery connected between the two superconductors can the Josephson current flow. No net current flows if a battery is connected because the current oscillates very quickly (F. Arnold, 2020). The Josephson Effect is affected by magnetic fields close to the superconductors, making it possible to monitor extremely weak magnetic fields.

The BCS hypothesis states that the correlated mobility of electrons in the superconducting material is what causes superconductivity. The development of electron pairs known as Cooper pairs contributes to this association. Josephson claims that under specific conditions, these Cooper pairs can penetrate the thin insulating layer from one superconductor to another. This type of electron pair movement is known as the Josephson current, and the method

through which the pairs pass through the insulating layer is known as Josephson tunnelling (J. Linder, 2019).

The superconducting quantum obstruction gadget (SQUID), a profoundly delicate identifier of attractive fields, relies upon the Josephson Effect to work. It is used to gauge minute differences in both the Earth's and the body's magnetic fields.

Complex order parameter is used to describe superconductors. For single-particle excitations from the ground state, the amplitude provides the energy gap. The gap manifests as a result of an energy cost for the emergence of an unpaired single electron imposed by an effective attraction between electrons, which can have several sources (K. Zuo, 2021). In a single homogenous superconductor, the phase of is irrelevant, but in the presence of a weak link, the phase difference may be sufficient to generate a super current. The Josephson Effect is evident here.

There are two ways that the Josephson Effect might appear: as a stationary effect (DC) and as a time-dependent effect (AC). The DC Josephson effect will be the sole thing we focus on. The dependency of the free energy on the superconducting phase difference across the junction is a complete description of this phenomena. According to the derivative, the super current is produced.

$$I\ (\emptyset) = \frac{2e}{h}\ \frac{dF}{d\emptyset} \qquad (1)$$

The critical current is the maximum value that a periodic function must have. At low temperatures, the dependency can be convoluted, but at high temperatures, all harmonics save the lowest one are suppressed, and we obtain the straightforward relationship.

$$I(\emptyset) = I_c\ \sin\emptyset \qquad (2)$$

The characteristics of the junction determine the size of the critical current.

4. FORMALISM OF SCATTERING MATRIX

Think about a Josephson junction (JJ), which frames a multi-terminal SNS contact when n superconducting (S) terminals are associated through the normal ordinary (N) district. To make the show as direct as could really be expected, we accept that both time-inversion and chiral balances are abused and that each superconducting lead is associated by only one directing direct in the typical region (unusual classes D and C) (L. Wu, 2018). Lucid Andreev

ISSN- 2394-5125 VOL 7, ISSUE 19, 2020

reflections that clarify the change of electrons for openings at the superconductor-typical connection point lead to the arrangement of the sub gap bound states in the JJs. A versatile dissipating occasion at energy in n-terminal junctions is distinguished by a dispersing grid S() U(2n), where 2 means the levels of opportunity for the molecule and opening. Following, we standardize all energy in units of and accept that all leads have the equivalent superconducting hole. The evenness of the molecule opening (PH) is addressed by

$$\widehat{S}(\mathcal{E}) = P\hat{S}(-\mathcal{E})P^{-1} \tag{3}$$

The determinant equation yields the Andreev bound-state energies.

$$Det[\|_{2n} - \hat{R}_{\wedge}(\mathcal{E}, \hat{\theta})\hat{S}_N(\mathcal{E})P^{-1} \tag{4}$$

Due to global gauge invariance, we set 0 to be 0. The block-diagonal forms of these scattering matrices result from the PH symmetry equation (3).

$$\hat{S}_N(\mathcal{E}) = \begin{bmatrix} \hat{s}_{(\mathcal{E})} & 0 \\ 0 & \hat{S}^* (-\epsilon) \end{bmatrix}$$

$$\hat{R}_{\wedge}(\varepsilon, \hat{\theta}) = e^{-i \arccos \varepsilon} \begin{matrix} 0 & e^{i\hat{\theta}} \\ -P^2_{e^{-i\hat{\theta}}} & 0 \end{matrix} \tag{5}$$

Further simplification results in a degree-n characteristic polynomial for the determinant in Equation (4). $\gamma(\varepsilon) \equiv e^{-2i \arccos \varepsilon}$,

$$P_n(\gamma; \hat{\theta}, \varepsilon) = Det\left[\|_n + P^2\gamma(\varepsilon)e^{i\hat{\theta}}S^*(-\epsilon)e^{-i\hat{\theta}}s(\varepsilon)\right] \tag{6}$$

Critically, from Eq. (6) that's what we see, for a decent typical locale dispersing grid ˆs, the Andreev groups of P2 = ±1 balance classes are double by means of the connection

$$\varepsilon^2_{p^2} = +1(\hat{\theta}) + \varepsilon^2_{p^2} = -1 = 1 \tag{7}$$

We previously provided a thorough explanation of the P2 = 1 condition and how it relates to three- and four-terminal junctions. The Andreev range of P2 = +1 junctions, which can sustain Majorana modes with zero energy, is the main subject of this review. To keep away from the effects of moving quasiparticles' impediment, we additionally expect energy-autonomous dispersing networks (s) that, for example, compare to points of failure when the junction's length is short comparative with the superconducting intelligence length, L (L. Yang, 2021). We bring up that this assumption isn't required for Majorana no modes to exist.

ISSN- 2394-5125 VOL 7, ISSUE 19, 2020

To concentrate on the energy spectra of rising states in junctions with terminals, we present the dispersing lattice as:

$$\hat{S}_0 \equiv \hat{R}_{\mathrm{A}}\left(0,\hat{\theta}\right)\hat{S}_N = i\begin{bmatrix} 0 & e^{-i\widehat{S^8}} \\ e^{-i\hat{S}} & 0 \end{bmatrix} \qquad (8)$$

which, in light of the fact that DetS0 = (1)n, is an individual from the round genuine outfit. By utilizing Eq. (4), the determinant condition of an antisymmetric framework m is utilized to compute the zero-energy Majorana modes,

$$Det\left[\widehat{m}\left(\hat{\theta}\right)\right] = 0, \;\; \widehat{m}\left(\hat{\theta}\right) = e^{-i\hat{\theta}/2}\hat{S}e^{i\hat{\theta}/2} - e^{i\hat{\theta}/2}\hat{S}^T e^{-i\hat{\theta}/2} \qquad (9)$$

We get huge characteristics from this. I Eq. (9) is commonly met for all dispersing frameworks and stages when n is odd. This recommends that Andreev-Majorana zero modes exist at all stages and are impervious to versatile dissipating and the nonuniformity of the superconducting request boundary. The Josephson flows are not impacted by these nondispersive level groups. The Pfaffian condition for n even determines the stages at which the Andreev groups intersect at zero energy.

$$Pf_{n\varepsilon even}\left[\widehat{m}\left(\hat{\theta}\right)\right] = 0. \qquad (10)$$

In light of our consideration of two- and four-terminal junctions, we predict that there are typically a few Majorana zero modes on a (n 2)-layered hypersurface in the = (1,...,n1) space addressed by Eq (10). The energy range of the connection is then revealed for different explicit dissipating framework designs.

5. MULTITERMINAL JOSEPHSON EFFECT

5.1. Junctions with two terminals

As a pattern, we initially research two-terminal junctions. We add four autonomous boundaries to the in pairs unitary lattice,

$$s = \begin{pmatrix} \sqrt{1 - Te^{i\varphi 00}} & \sqrt{Te^{i\varphi 01}} \\ \sqrt{Te^{i\varphi 10}} & \sqrt{1 - Te^{i\varphi 01 + \varphi 10 - \varphi 00}} \end{pmatrix} \qquad (11)$$

The two parts of dispersive arrangements are given by

$$\varepsilon(\upsilon) = \pm \begin{Bmatrix} \sqrt{T\cos(\upsilon/2} \\ \sqrt{1 - T\,sin^2(\upsilon/2)} \end{Bmatrix} \qquad \begin{matrix} P^2 = +1, \\ P^2 = -1, \end{matrix} \qquad (12)$$

ISSN- 2394-5125 VOL 7, ISSUE 19, 2020

Where for correlation we review the outcomes for the regular P2 = −1 junctions.

$$J(\upsilon) = \pm\frac{e\Delta}{\hbar} \times \begin{Bmatrix} \sqrt{T}\sin(\upsilon/2) \\ T\sin\upsilon/4\varepsilon(\upsilon) \end{Bmatrix} \quad \begin{matrix} P^2 = +1, \\ P^2 = -1, \end{matrix} \qquad (13)$$

The bound states are isolates from the continuum with an insignificant hole.

5.2. Three-terminal junctions

With n = 3, the range that the palindromic polynomial confines is still undefined and made up of three groups.

$$\varepsilon_{\pm}(\theta) = \pm\sqrt{\frac{1-B_3(\theta)}{2}}, \qquad \varepsilon_0(\theta) = 0 \qquad (14)$$

Taking on a similar parametrization of the dispersing grid as in Ref. [34], the B3 capability can be tracked down in the shut scientific structure

$$B_3 = \frac{1}{2}\Big[2a^2 - (1+a^2)b^2 + c^2 - 2b^2c^2 - 4abc\sqrt{(1-b^2)(1-c^{2)}}cos\boldsymbol{\varphi}\Big] + bc(1 - a^2)\cos\upsilon_1 + (1-a^2)\sqrt{(1-b^2)(1-c^2)cos}\upsilon^2 + \Big[bc(1+a^2)\sqrt{(1-b^2)(1-c^2) + a(b^2+c^2-2b^2c^2)cos}\boldsymbol{\varphi}\Big] \times \cos(\upsilon_{1-}\upsilon_2) + a(b^2-c^2)sin\boldsymbol{\varphi}\sin(\upsilon_{1-}\upsilon_2). \qquad (15)$$

Thus, there are just six autonomous boundaries of the dissipating lattice that enter the range of Andreev bound states.

5.3. Four-terminal junctions

Majorana zero modes and Weyl hubs can coexist in the energy range of four-terminal junctions.

$$\varepsilon(\theta) = \pm\sqrt{\frac{4-A_4\pm\sqrt{A_4^2-4B+8}}{8}}, \qquad (16)$$

6. MODEL

We consider two superconducting districts that are portrayed as firmly doped Weyl semimetals, otherwise called "Weyl metals," with superconducting request, sandwiched between a piece of ordinary Weyl (semi)metal with two Weyl purposes of restricting chirality

ISSN- 2394-5125 VOL 7, ISSUE 19, 2020

at momenta. We can accept, without losing over-simplification, that the Weyl focuses are situated in the px-pz plane.

$$h_{\pm}(q) = hv[q_1\sigma_1 + q_2\sigma_2 \mp q_3\sigma_3 + V_0\theta\left(|z| - \frac{L}{2}\right) - \mu, \quad (17)$$

where v is the Fermi speed, μ the synthetic potential,

$$q_1 = q_x \cos cx - q_z \sin cx,$$

$$q_2 = q_y,$$

$$q_3 = q_z \cos cx + q_x \sin cx \quad (18)$$

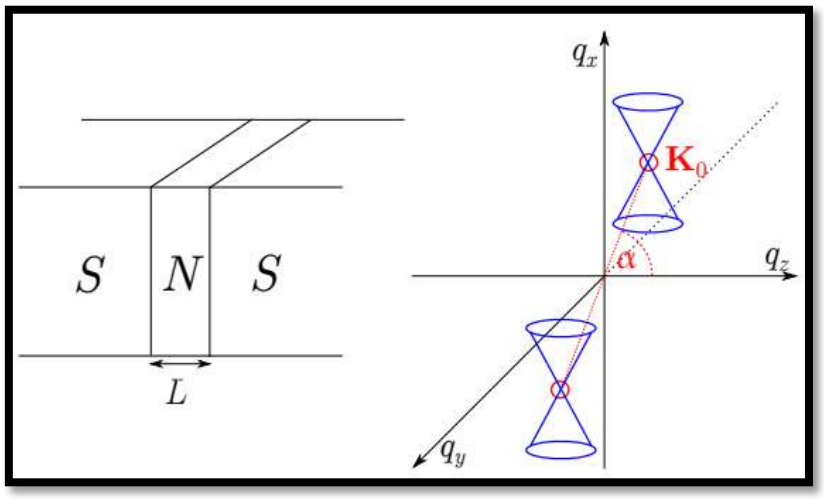

Figure 2: (Left) A chart of the math being concentrated Between two doped, Outline of the energy space (right) showing two "Weyl cones" at momenta K0.

There are two potential superconducting pairings in Weyl semimetals. The Cooper matches join electrons from Weyl focuses with the contrary chirality while having zero energy and twist for the BCS-like matching. The Cooper matches for the FFLO-like matching are comprised of two electrons with the indistinguishable chirality and have zero twist and limited energy 2K0. Given that various models contend that the matched state that is similar to the BCS is the superconducting ground state, we should take into account both matching structures, in spite of the way that the FFLO-like matching is vivaciously worthwhile for a grid model with feeble appealing cooperations hidden the continuum Hamiltonian (O. V. Gamayun, 2022). The decadence between the two Weyl focuses might be lifted on the off chance that both time-inversion evenness and reversal balance are broken, and the main matching structure allowed by balance is the FFLO-like matching.

ISSN- 2394-5125 VOL 7, ISSUE 19, 2020

The potential offset V0 for the superconducting is huge and negative in order to maintain the linearized depiction around each Weyl cone.

The superconductor's excitation range is gapped for FFLO-like matching, with excitation hole,

$$\Delta_F = \Delta_0, \tag{19}$$

The two superconducting zones become "Weyl superconductors" when the quasiparticle range in both of them has two hubs for BCS-like matching.

$$\Delta_B = \Delta_0 \, |\sin cx|; \tag{20}$$

7. RESULTS

We show discoveries for the Josephson current thickness standardized by the junction's ordinary state conductivity N. The Landauer equation is utilized to decide the ordinary state conductivity, which is characterized as the conductance per unit cross-sectional region.

$$\sigma_N = \frac{2e^2}{h} \int \frac{dq_x dq_y}{(2\pi)^2} T(q_x, q_y) \tag{21}$$

where the probability of transmission

$$T(q_x, q_y) = \frac{q_z^2}{q_z^2 + q_\perp^2 \, sin^2(q_2 L)}, \tag{22}$$

By using the junction, it is possible to distinguish between two types of transport systems: those that are dominated by spreading modes or by transitory modes. In the above scenario, where one has ||L/v1, the requirement in Eq. (21) that corresponds to genuine qz is required. At the intersection, conduction is

$$\sigma_N = \frac{\mu^2 e^2}{6\pi^2 h^3 v^2} \tag{23}$$

In the last option case the vital in Eq. (21) compares to fanciful qz, and the junction conductivity is

$$\sigma_N = \frac{e^2 \ln 2}{2\pi^2 h L^2} \tag{24}$$

The information displayed above and in the past segment can be utilized to figure the Josephson current thickness, meant by j(φ). Except for the high-temperature limit, we

ISSN- 2394-5125 VOL 7, ISSUE 19, 2020

couldn't execute the combinations over the cross over momenta qx and qy in shut structure. for which we find

$$j_{F,B}(\emptyset) = \frac{\Delta_{F,B}^2 \sigma N}{2\pi e k_B T} \sin \emptyset \qquad (25)$$

Notwithstanding the immeasurably various conductivities in the two systems [compare Eqs. (23) and (24)],

8. DISCUSSION

In this paper, we utilized dissipating framework hypothesis procedures to analyze the transport qualities of topological superconductors' multiterminal Josephson junctions. We have focused on the spectrum of subgap states and found that the surface of the following Andreev groups in the multifaceted border space of superconducting stages can lead to nonvanishing motions of the Berry ebb and flow in two-, three-, and four-terminal arrangements. These highlights immediately lead to the quantized nonlocal conductances of these devices. Furthermore, we have taken a gander at the cooperations and current-stage connections of supercurrents as well as their mesoscopic measurable qualities (R. M. Lutchyn, 2021). We explicitly covered the topological system's ongoing cross-relationship capability and supercurrent change notwithstanding the all inclusive system of current variances. We conclude this work with a few remarks on momentum and prospective future research that could also look into the unexplored physical science of multiterminal Josephsonic devices.

Josephson's super currents and conductance’s have recently been used to calculate the surface states of nearby superconducting planar junction devices and topological claddings as a function of temperature and input voltage to understand the concept of electron transport in these frameworks. We find that the super current as a component of the door voltage exhibits an unexpected drop, superimposed with repeatable noise whose value is a small fraction of the background current. To understand the precise pattern of underlying current dependence, the component associated with the shift of surface topological states relative to the dilute dominant bilayer state generated by the near-surface banding strip was used. By pushing the unrelated states under the topological surface states, negative gating potentials in real space revealed the disordered surface topological states of TI. As a result, the strength of the supercurrent fluctuates greatly (S.-Y. Xu, 2021). The seepage effect has been attributed to the fuss. This is because nearby charge fluctuations near voltage edges can unnecessarily wander

ISSN- 2394-5125 VOL 7, ISSUE 19, 2020

the supercurrent curve. Given that this excitement can begin mesoscopically, we must hint at the possibility of a surrogate situation. In this case, the indistinguishable and reproducible oscillation properties of the Fraunhofer magnetomotion assigned to the background current are even more useful. Despite the fact that our model cannot be directly applied to S-TI-S interconnections, the number of variants present proves to be consistent with the theory that elimination of the problem causes the observed mesoscopic effect. understand.

Also note that circuit swapping can be used to highlight relevant facts of superflow. The supercurrent solves the Majorana fermion (consistent) equation condition in the transition to the Majorana mode, sin(/2), especially since the fundamental current estimate of the topological Josephson device gives the odd fraction part There is a possibility. Select where characters encode equivalences. Exchange estimation is usually performed by adjusting the slope current through the junction to determine the successive values at which the junction enters a finite voltage state. . One hopes to find a bimodal conveyance showing the two equality states by over and over executing this convention and gathering measurements of irregular supercurrent exchanging occasions (as beforehand effectively finished in a few mesoscopic closeness circuits). One can distinguish the equality state (with some devotion) assuming the distance between the two tops in this appropriation is sufficiently huge. Our transport hypothesis will be useful in recreating forthcoming estimations (Murakami, 2021). The multiterminal gadgets thought about in this work can offer a real equipment stage for leading such tests. Specifically, sorting out the energy hindrance of a stage slip that starts the exchanging requires information on the current-stage association. Likewise, the conceivable utilization of multiterminal gadgets in the development of safeguarded superconducting qubits fills in as motivation for these advancements.

9. CONCLUSION

In this article, we evaluated the Josephson current through a thin mass of Weyl (semi) metal under standard conditions. We studied matching systems of superconductors similar to both BCS and FFLO, modeling the superconducting terminals as heavily doped Weyl metals. Weyl semimetals are known to exhibit highly peculiar transport properties at the Weyl point = 0. The conductance of the cubic example is essentially sizeless under normal conditions and scales approximately to W2/L2 for tests of width W and length L. 50,51 (In contrast, in the cubic example, the conductivity of ordinary diffusive metals is related to L on three sides.) The Josephson effect is also the effect of this atypical scaling on the frame size L

receive. Relative values of the Josephson current scale to the normal-state conductance over the limit range we investigated. This result is consistent with the short junction limit used in our calculations given the usual energy of the Andreev binding term mediating the Josephson current.

REFERENCES

1. *A. A. Burkov, Jounal of Phys. Cond. Matt. 27, 113201 (2020); A. Turner and A. Vishwanath, arXiv:1301.0330 (unpublished); P. Hosur and X. Qi, Comptes Rendus Physique, 14, 857 (2013); S.Rao, arXiv:1603.02821 (unpublished); W. Witczak-Krempa, G. Chen, Y. B. Kim, and L. Balents, Ann. Rev. Cond. Mat. 5, 57 (2019).*
2. *A. Das, Y. Ronen, Y. Most, Y. Oreg, M. Heiblum, and H. Shtrikman, Evidence of Majorana fermions in an Al-InAs nanowire topological superconductor, Nat. Phys. 8, 887 (2020).*
3. *C.W. J. Beenakker, N. V. Gnezdilov, E. Dresselhaus, V. P. Ostroukh, İ. Adagideli, and J. Tworzydło. Valley switch in a graphene superlattice due to pseudo-Andreev reflection. arXiv:1805.02487.*
4. *D. Sherman, J. S. Yodh, S. M. Albrecht, J. Nygard, P. Krogstrup, and C. M. Marcus, Hybrid Double Quantum Dots: Normal, Superconducting, and Topological Regimes, Nat. Nanotechnol. 12, 212 (2022).*
5. *E. M. Spanton, M. Deng, S. Vaitiekenas, P. Krogstrup, J. Nygard, C. M. Marcus, and K. A. Moler, Current-phase relations of few-mode InAs nanowire Josephson junctions, Nat. Phys. 13, 1177 (2022).*
6. *F. Arnold, C. Shekhar, S.-C. Wu, Y. Sun, R. D. Dos Reis, N. Kumar, M. Naumann, M. O. Ajeesh, M. Schmidt, A. G. Grushin, J. H. Bardarson, M. Baenitz, D. Sokolov, H. Borrmann, M. Nicklas, C. Felser, E. Hassinger, and B. Yan, Nat. Commun. 7, 11615 (2020).*
7. *J. Linder, A. M. Black-Schaffer, T. Yokoyama, S. Doniach, and A. Sudbø, Phys. Rev. B 80, 094522 (2019)*
8. *K. Zuo, V. Mourik, D. B. Szombati, B. Nijholt, D. J. van Woerkom, A. Geresdi, J. Chen, V. P. Ostroukh, A. R. Akhmerov, S. R. Plissard, D. Car, E. P. A. M. Bakkers, D. I. Pikulin, L. P. Kouwenhoven, and S. M. Frolov. Supercurrent interference in few-mode nanowire Josephson junctions. Phys. Rev. Lett. 119, 187704 (2021).*

9. *L. Wu, M. Brahlek, R. V. Aguilar, A. Stier, C. Morris, Y. Lubashevsky, L. Bilbro, N. Bansal, S. Oh, and N. Armitage, Nat. Phys. 9, 410 (2018); F.D.M Haldane, arXiv:1401.0529; I. Belopolski, et al., Phys. Rev. Lett. 116, 066802 (2020).*
10. *L. Yang, Z. Liu, Y. Sun, H. Peng, H. Yang, T. Zhang, B. Zhou, Y. Zhang, Y. Guo, M. Rahn, D. Prabhakaran, Z. Hussain, S.-K. Mo, C. Felser, B. Yan, and Y. Chen, Nat. Phys. 11, 728 (2021).*
11. *Li, B., Wang, Q., Xu, Y., & Yang, Y. (2021). Andreev reflection and Josephson effect in Weyl semimetal/superconductor hybrid junctions. Physical Review B, 103(7), 075422. doi:10.1103/PhysRevB.103.075422*
12. *O. V. Gamayun, V. P. Ostroukh, N. V. Gnezdilov, İ. Adagideli, and C.W. J. Beenakker. Valley-momentum locking in a graphene su- perlattice with Y-shaped Kekulé bond texture. New J. Phys. 20, 023016 (2022)*
13. *R. M. Lutchyn, E. P. A. M. Bakkers, L. P. Kouwenhoven, P. Krogstrup, C. M. Marcus, and Y. Oreg, Realizing Majorana zero modes in superconductor-semiconductor heterostructures, Nat. Rev. Mater. 3, 52 (2021).*
14. *R. Okugawa and S. Murakami, Phys. Rev. B 96, 115201 (2021)*
15. *S.-B. Zhang, F. Dolcini, D. Breunig, and B. Trauzettel, Phys. Rev. B 97, 041116(R) (2019); D. K. Mukherjee, S. Rao, and A. Kundu, Phys. Rev. B 96, 161408(R) (2020); U. Khanna, S. Rao, and A. Kundu, ibid. 95, 201115(R) (2020); U. Khanna, D. K.Mukherjee, A. Kundu, and S. Rao, ibid. 93, 121409(R) (2019); M. Alidoust and K. Halterman, arXiv:1906.05382 (unpublished); M. Alidoust, Phys. Rev. B 98, 245418 (2019); M. Alidoust, K. Halterman, and A. A. Zyuzin, Phys. Rev. B 95, 155124 (2020)*
16. *S.-Y. Xu, N. Alidoust, I. Belopolski, C. Zhang, G. Bian, T.-R. Chang, H. Zheng, V. Strokov, D. S. Sanchez, G. Chang, Z. Yuan, D. Mou, Y. Wu, L. Huang, C.-C. Lee, S.-M. Huang, B. Wang, A. Bansil, H.-T. Jeng, T. Neupert, A. Kaminski, H. Lin, S. Jia, and M. Z. Hasan, Nat. Phys. 11, 748 (2021).*
17. *Wu, F., & Das Sarma, S. (2020). Josephson effect in Weyl semimetal-superconductor hybrid structures. Physical Review B, 101(18), 184505. doi:10.1103/PhysRevB.101.184505*
18. *Zhang, J., Wu, Y., Liu, Z., Wang, Q., & Yang, Y. (2020). Josephson effect and Majorana zero modes in topological superconductor/Weyl semimetal heterostructures. Physical Review B, 101(15), 155424. doi:10.1103/PhysRevB.101.155424*

19. *Zhang, X., & Law, K. T. (2020). Josephson effect in Weyl semimetal junctions. Physical Review B, 102(20), 205417. doi:10.1103/PhysRevB.102.205417*
20. *Zhang, X., & Law, K. T. (2021). Proximity-induced unconventional Josephson effect in Weyl semimetal-based SNS junctions. Physical Review B, 103(3), 035437. doi:10.1103/PhysRevB.103.035437*

*****